

# Research on biogenesis of mitochondria in astrocytes in sepsis-associated encephalopathy models

Y.-Z. ZHAO<sup>1</sup>, Z.-Y. GAO<sup>2</sup>, L.-O. MA<sup>1</sup>, Y.-Y. ZHUANG<sup>3</sup>, F.-L. GUAN<sup>4</sup>

<sup>1</sup>Department of Neurosurgery, Hongqi Hospital Affiliated to Mudanjiang Medical College, Mudanjiang, Heilongjiang Province, China

<sup>2</sup>Department of ICU Care, Hongqi Hospital Affiliated to Mudanjiang Medical College, Mudanjiang, Heilongjiang Province, China

<sup>3</sup>Medical Insurance Section, Hongqi Hospital Affiliated to Mudanjiang Medical College, Mudanjiang, Heilongjiang Province, China

<sup>4</sup>Department of Outpatient Surgery, Hongqi Hospital Affiliated to Mudanjiang Medical College, Mudanjiang, Heilongjiang Province, China

**Abstract. – OBJECTIVE:** To study the structural and functional changes in mitochondria in astrocytes of the cerebral cortex of the rats in the simulated sepsis environment *in vitro* and the relationship between these changes and the biogenesis of mitochondria in astrocytes by establishing models of sepsis astrocytes.

**MATERIALS AND METHODS:** The structural and functional changes in mitochondria in astrocytes of the cerebral cortex of the rats were evaluated. The ultra structural changes in the mitochondria, astrocytes, and ultrathin sections, were observed with a transmission electron microscope. The expression of the regulatory factors related to biogenesis of mitochondria in astrocytes of the cerebral cortex of the rats was evaluated in various experimental groups. RT-PCR and Western blot were used to evaluate the expression of the regulatory factors related to biogenesis of mitochondria in astrocytes of the cerebral cortex of the rats. The “point grid method” was used to evaluate the volume density of the mitochondria in the astrocytes of the cerebral cortex of the rats in various experimental groups. The Western blotting was used to evaluate the role of fusion and fission of mitochondria in the astrocytes of the cerebral cortex of the rats in various experimental groups in regulating the expression of the protein-OPAI and DRPI.

**RESULTS:** In the sepsis astrocyte models established by co-incubation of LPS and IFN- $\gamma$  and astrocytes of the cerebral cortex of the rats, the mitochondria with a minor injury in the 6 h group ( $2.97 \pm 0.92$ ) increased significantly when compared with those in the 0 h group ( $1.08 \pm 0.95$ ), 12 h group ( $1.70 \pm 1.01$ ), and 24 h group ( $1.59 \pm 0.55$ ) ( $p < 0.05$ ); the concentration

of adenosine triphosphate (ATP) in the astrocytes of the cerebral cortex of the rats in the 6 h, 12 h, and 24 h groups increased significantly when compared with that in the 0 h group ( $p < 0.05$ ). PGC-1 $\alpha$  mRNA, NRF-1 mRNA, NRF-2 $\alpha$  mRNA, NRF-2 $\beta$  mRNA, and mitochondrial transcription factor A (TFAM) mRNA in the astrocytes of the cerebral cortex of the rats in the 6 h and 12 h groups increased significantly when compared with those in the 0 h group ( $p < 0.05$ ); the concentration of TFAM mRNA ( $1.20 \pm 0.19$ ) increased significantly when compared with that in the 0 h group ( $p < 0.05$ ). The OPAI protein concentration ( $1.21 \pm 0.17$ : $1.34 \pm 0.06$ ) and DRPI protein concentration ( $1.04 \pm 0.05$ ;  $1.05 \pm 0.05$ ) in the astrocytes of the cerebral cortex of the rats in the 12 h group ( $1.25 \pm 0.17$ ), 24 h group ( $1.33 \pm 0.24$ ), and 6 h group increased significantly when compared with that in the 0 h group ( $p < 0.05$ ).

**CONCLUSIONS:** The experimental sepsis conditions can cause a minor injury of the ultrastructure of the mitochondria in the astrocytes of the cerebral cortex of the rats. The biogenesis of the mitochondria in the astrocytes of the cerebral cortex of the rats was strengthened to cater for the increased demand for energy of the astrocytes under the sepsis conditions and finally recover the ultrastructure of the mitochondria with a minor injury. In response to the increased mitochondrial biogenesis, the activities of the mitochondrial fusion and fission of the astrocytes of the cerebral cortex of the rats were increased.

Key Words:

Sepsis, Sepsis-associated encephalopathy, Astrocytes, Mitochondrial biogenesis.

## Introduction

The cerebral dysfunction caused by sepsis is called sepsis associated encephalopathy (SAE). SAE is a disseminated cerebral dysfunction, caused by sepsis-induced systemic inflammatory responses, characterized by such clinical or laboratory bases as no central nervous system infection, abnormal cerebral anatomical structure, cerebral hemorrhage or cerebral embolism, etc.<sup>1-3</sup>. SAE seriously influences the prognosis of the sepsis patients. SAE has become an independent factor for predicting the death of sepsis patients<sup>4</sup>. The SAE survivors often suffer from acute or chronic autonomic nerve dysfunctions, delirium or damaged cognitive functions of different degrees<sup>5</sup>. Also, SAE can influence the functions of other important organs and accelerate the occurrence and progression of the sepsis-related multiple organ dysfunction syndrome by influencing the functions of the automatic nervous system and the neuroendocrine system due to the specificity of the cerebral functions<sup>6-8</sup>. The pathogenesis of SAE is very complex and not completely clear. Thus, discussing the molecular mechanism of onset is significant to prevention and treatment of SAE and improving the prognosis of the patients with sepsis and multiple organ dysfunction syndrome. Previous studies<sup>9,10</sup> have found that the mitochondrial dysfunction is closely associated with the damage to the energy supply for the brain tissue cells and the increase in neurocytes apoptosis; it can exacerbate the sepsis-induced cerebral dysfunctions; it has become one of the major pathogenesis of SAE<sup>11-13</sup>. The mitochondrial biogenesis is subject to dual regulation by the regulatory factors related to cell nucleus and mitochondria biogenesis<sup>14,15</sup>. Mitochondrial biogenesis: the growth and differentiation of the existing mitochondria achieve dual regulation of the mitochondrial biogenesis including brain tissue by regulatory factors related to cell nuclei and mitochondria<sup>16-18</sup> by expressing, infusing and assembling the cell nuclei and mitochondrial encoded mitochondrial protein and regulating the content and morphology of the mitochondria. However, there is no systematic research on the effect of biogenesis of the brain tissue mitochondria in the course of sepsis. The astrocytes can strengthen the formation of functional synapses in the central nervous system and maintain the stability of the synapses, regulate synaptic transmission and neurogenesis, transform into nervous stem/progenitor cells, develop a blood brain barrier, induce formation of the blood brain barrier and maintain its functions, regulate cerebral blood flow, synaptic interstitial fluid, ionic concentration, pH value, and

neurotransmitter steady state, energy and metabolism of the central nervous system<sup>19</sup>. In the inflammatory reactive diseases, the reactive astrocytes aggregate in the vicinity of the brain abscess arising from pathogenic microorganisms. As multifunction cells of the central nervous system, the dysfunctions of the astrocytes are closely associated with the neurocyte and cerebral dysfunctions<sup>20</sup>. Normal mitochondrial functions of the astrocytes are an important guarantee for the astrocytes to exert normal functions. Studying the changes in the mitochondrial biogenesis of the astrocytes in the course of sepsis is positively significant to the understanding of the physiological and pathological processes of SAE.

## Materials and Methods

### Materials and Reagents

This study was approved by the Animal Ethics Committee of Mudanjiang Medical College Animal Center. The SPF neonatal SD rats (aged one day, Laboratory Animal Center of Mudanjiang Medical College); gram-negative bacterium lipopolysaccharide (LPS) (Sigma-Aldrich, St. Louis, MO, USA); recombinant rat interferon- $\gamma$  (IFN- $\gamma$ ) (Life Technology, Carlsbad, CA, USA); mouse anti-rat glial fibrillary acidic protein (GFAP) monoclonal antibody (Cell Signaling Technology, Danvers, MA, USA); rabbit anti-rat Iba-1 polyclonal antibody (Wako Pure Chemical Industries, Osaka, Japan); tumor necrosis factor- $\alpha$  ELISA kit (Neobioscience Biotechnology Co., Ltd., Shenzhen, China); interleukin-6 ELISA kit (Neobioscience Biotechnology Co., Ltd., Shenzhen, China); nitric oxide detection kit (Beyotime Biotechnology Research Institute, Nanjing, China); dichlorodihydrofluorescein diacetate (DCFDA) cell viability chalcogen kit (Abcam, Cambridge, MA, USA); goat anti-rat PGC-1 $\alpha$  polyclonal antibody, rabbit anti-rat OPAI monoclonal antibody (Abcam, Cambridge, MA, USA); rabbit anti-rat NRF-1 polyclonal antibody, rabbit anti-rat NRF-2 $\alpha$  polyclonal antibody, rabbit anti-rat NRF-2 $\beta$  polyclonal antibody, goat anti-rat mitochondrial transcription factor A (TFAM) polyclonal antibody (Abcam, Cambridge, MA, USA); goat anti-rat DRP1 polyclonal antibody (Santa Cruz Biotechnology, Santa Cruz, CA, USA). Instrumentation and equipment: SpectraMaxM5 Multi-functional microplate reader (GE MDS, Rochester, NY, USA); ABI7500 fluorescent quantitation PCR amplifier (Applied Biosystems ABI, Foster City, CA, USA); Olympus 1 $\times$ 71 inverted fluorescence microscope, Olympus Sz61 stereoscopic microscope (Olympus, Tokyo, Japan); H7650 tran-

mission electron microscopy (Hitachi, Tokyo, Japan); Kodak Image station 4000R/Pro fluorescence/chemiluminescence/*in vivo* isotope imaging analysis system (Kodak, Rochester, NY, USA).

#### **Preparation of Sepsis Astrocyte Models**

The LPS (50 ng/mL) working solution and IFN- $\gamma$  (200 U/ml) working solution were co-incubated with the astrocytes of the cerebral cortex of the rats and the stimulus response of the sepsis to the astrocytes was simulated in the *in vitro* environment. The rats were divided into 4 experimental groups: 0 h group, normal control group, 6 h group, 12 h group, 24 h group.

#### **Culturing the Astrocytes**

The cerebellum, meninges, large vessels, cerebral medullary substance, and cerebral cortex of the neonatal Sprague Dawley (SD) rat aged 1 day were carefully separated with a pair of microsurgery tweezers under the dissecting microscope. The complete separated cerebral cortex was gently cut into tissue blocks with a volume about 1 mm<sup>3</sup> with a surgical knife blade. The tissue blocks were filtered, inoculated in the cell suspension, and placed in an incubator containing 5% carbon dioxide at 37°C. The solution was changed once by negative pressure suction with low-sugar Dulbecco's Modified Eagle Medium (DMEM) containing 10% fetal bovine serum (FBS) and 0.15% penicillin-streptomycin mixture at 24 h after the tissue blocks were inoculated in the cell suspension. The tissue blocks were used after at 4 weeks after culturing<sup>21</sup>.

#### **Concentration Measurement of TNF- $\alpha$ and IL-6**

The batters were taken from the sealed bag, which had been balanced to room temperature. The standards and specimen diluent was added to the blank wells. Specimens or standards (100 pl/well) of different concentrations were added to the appropriate corresponding wells. The reaction wells were sealed with adhesive tape. It was incubated for 90 min at 36°C. The biotinylated antibody diluent was added to the blank wells after it was washed for 5 times. The biotinylated antibody working solution was added to other wells (100 pl/well). The reaction wells were sealed with the new batters. The solution was incubated for 60 min at 36°C. The enzyme combination dilute was added to the blank wells after it was washed 5 times. The enzyme combination working solution was added to other wells (100 pl/well). The cells were incubated in the incubator for 30 min at 36°C after the reaction wells were sealed with

adhesive tape. The chromogenic substrate was added after it was washed 5 times. The OD450 value was measured with the multi-functional microplate reader after the solution was well mixed.

#### **Concentration Measurement of ROS and NO**

The astrocytes inoculated into the 96-well microplate were washed carefully with PBS. The cells were incubated at 37°C for 45 min in darkness after the addition of the DCFDA mixture; the fluorescence intensity of each well was detected. The data were stored in the instrument.

#### **Ultrastructure of the Mitochondria in the Astrocytes**

The glutaraldehyde osmic acid double fixation method was used. The specimen was washed with acetic acid and barbital buffer solution, dehydrated, soaked, embedded, and aggregated. The ultrathin sections were stained for 30 min with uranyl acetate, and washed 3 times with distilled water. The water on the surface of the ultrathin sections was absorbed with filter paper and air-dried. The ultrathin sections were stored in a copper net box for observation.

#### **Volume Density of the Mitochondria**

Volume density of the mitochondria in the astrocytes of the cerebral cortex of the rats in various experimental groups was calculated using the "point grid method" according to a previous work<sup>22</sup>. The computational method was as follows: the transparent grids prepared with the above method were placed on the transmission electron microscope images of the astrocytes of the cerebral cortex. Additionally, the crosses of the transparent grid horizontal and vertical lines on the mitochondria of the astrocytes on the image were counted (excluding the junction points of the horizontal and vertical lines of the transparent grid on the four margins of the image).

#### **Concentration of ATP**

The culture solution in the 6-well microplate containing the astrocytes of the cerebral cortex of the rats was pipetted. 200  $\mu$ L ATP lysis buffer was added to each well. The solution was pipetted up and down thus enabling the lysis solution to sufficiently contact and decompose the astrocytes. The decomposed astrocytes were collected in a 1.5 mL centrifuge tube and centrifuged at 12000 $\times$ g for 10 min at 4°C. The supernatant was removed. 100  $\mu$ L ATP working solution was

added to each well. It was allowed to stand still for 5 min for complete consumption of ATP 80  $\mu$ L of the specimen or standard was added to the inspection hole. It was well mixed quickly with the pipette. The IUU value was determined with the multi-function microplate reader at 2 s. The ATP concentration in the sample was calculated in accordance with the standard curve.

### **RT-qPCR and Western Blot**

Real-time quantitative polymerase chain reaction (detecting the levels of related proteins with RT-PCR and Western-blot) was performed according to a previous work<sup>23</sup>. The sequence of the primers was showed in Table I.

### **Statistical Analysis**

The SPSS 16.0 statistical software (SPSS Inc., Chicago, IL, USA) was used for statistical analysis. The measurement data were expressed with mean  $\pm$  standard deviation ( $\bar{x}\pm$ sd). The comparison of mean among various groups used the analysis of variance. The homogeneity test of variance was conducted first. The Welch test would be used in the case of heterogeneity of variance. Pairwise comparisons were conducted among various mean. The least-significant difference (LSD) was used in the case of homogeneity of variance, and the Dunnett'T3 method was used in the case of heterogeneity of variance. The difference was considered statistically significant when  $p<0.05$ .

## **Results**

### **Purity Identification for the Primary Astrocytes**

The specific protein GFAP in the astrocytes and the specific protein Iba-1 in the microglial cells were marked with the immunocytochemical method; the morphology of the cells was observed.

The astrocytes accounted for more than 95% of the primary cells cultured and the microglial cells accounted for less than 5%. The results complied with the experimental requirements (Figure 1).

### **Concentrations of ROS in Astrocytes and TNF- $\alpha$ , IL-6, and NO in Sepsis**

The heterogeneity of variance occurred to the TNF- $\alpha$  concentration in various experimental groups. The TNF- $\alpha$  concentration in 3 h group, 6 h group, 12 h group, and 24 h group increased significantly when compared with that in the control group. The difference was statistically significant ( $p<0.05$ ). The concentrations of IL-6, ROS, and NO in 3 h group, 6 h group, 12 h group, and 24 h group increased significantly when compared with that in the control group. The difference was statistically significant ( $p<0.05$ ) (Figure 2).

### **Ultrastructure of the Mitochondria in the Astrocytes.**

In the models of sepsis astrocytes established by co-incubation of the LPS and IFN- $\gamma$  and the astrocytes of the cerebral cortex of the rats, we observed the ultrastructure of the mitochondria in the astrocytes of the cerebral cortex of the rats with the transmission electron microscope. It was found that the mitochondria with a mildly damaged ultrastructure (mitochondria with the ultrastructure score of 1 point) in the 6 h group increased significantly when compared with those in the 0 h, 12 h, and 24 h groups; there was no significant difference in percentages in various experimental groups between the mitochondria with a normal ultrastructure (the mitochondria with the ultrastructure score of 0 point) and the mitochondria with a mildly damaged ultrastructure (the mitochondria with the ultrastructure score of 2 points); no mitochondria with a severely damaged ultrastructure and extremely seriously damaged ultrastructure (the mitochondria with the ultra-

**Table I.** The sequence of the primers.

Gene	Primer Sequence (5'-3')	Annealing Temperature (oC)	Product Length (bp)
PGC-1a	TGAAGCTTGAATAGTCACG	63.6	90
NRF-1	CTGGCTAGTGCATTAG	60.0	115
NRF-2a	GGGGTCATGCATTTCA	60.0	120
NRF-2b	CTCAGTCGGTCAGTCC	60.0	72
TFAM	TGAGCTAGGTGCCGTGTG	64.3	146
B-actin	GACAGGATGCAGAAGATT	58	142
ND1	CCCAACATCGTAGTCATG	61.83	130
LPL	CTCCTAGTCAGTCGAGTCGAT	61.22	100



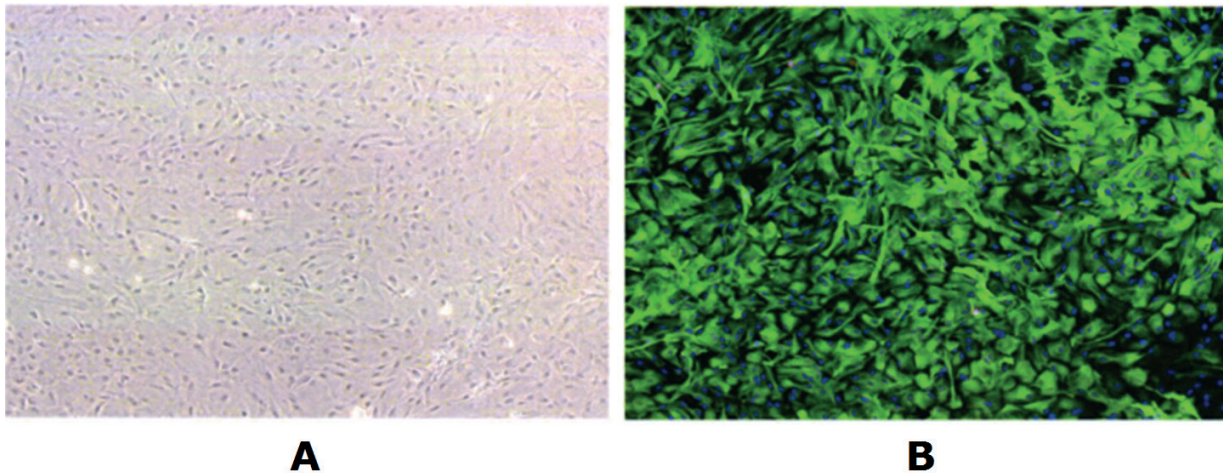


**Figure 1.** Purity identification for the primary astrocytes of the cerebral cortex of the rats. **A**, The astrocytes had abundant cytoplasm, irregular soma, and long and thin processes, which interlaced to form a network. The oval-shaped cell nuclei were usually inclined to one side (magnification  $\times 10$ ); **B**, The green color represents the astrocytes with positive expression of specific protein GFAP; the red color represents the microglial cells with positive expression of the specific protein Iba-1; the blue color represents the cell nuclei stained with DAPI (magnification  $\times 10$ ).

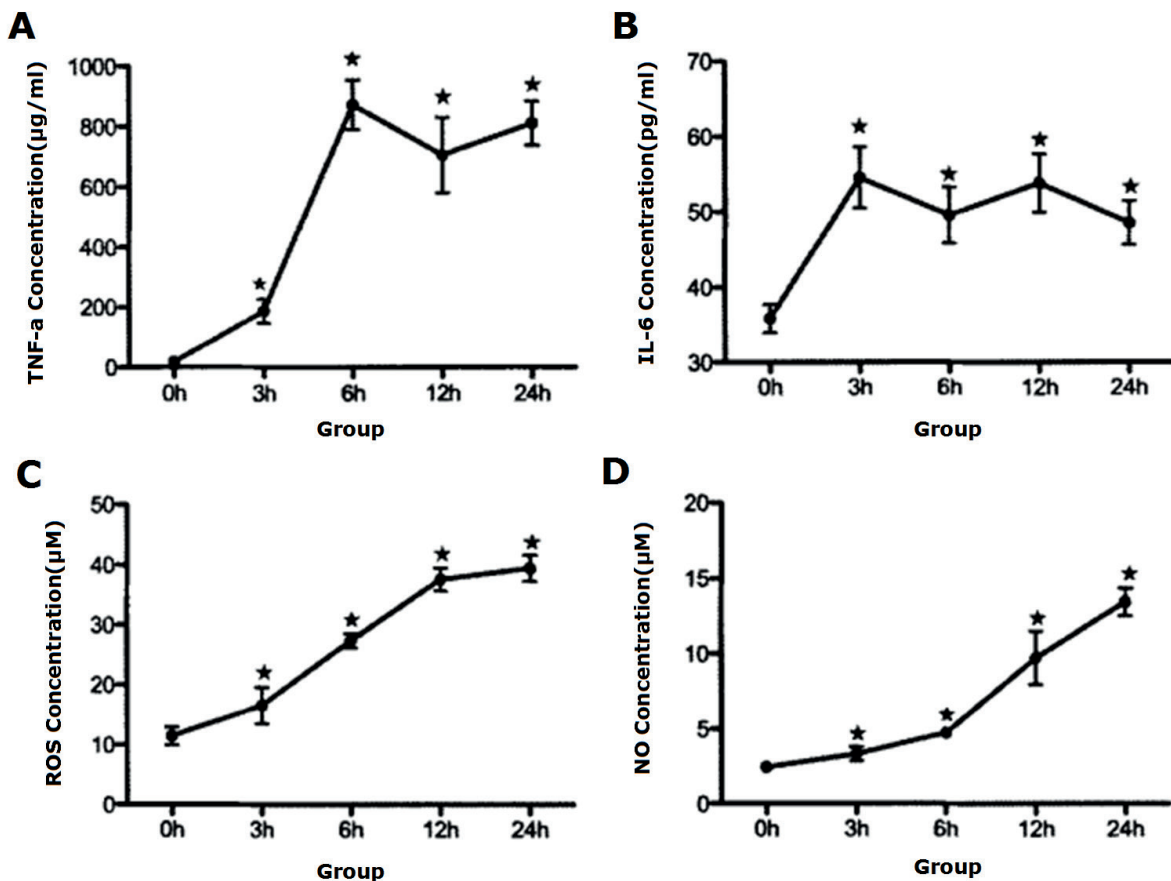


**Figure 2.** Comparison of concentrations of biomarkers in sepsis ( $\bar{x} \pm s$ ). **A**, The TNF- $\alpha$  concentration in 3 h, 6 h, 12 h, and 24 h groups increased significantly when compared with that in the control group; **B**, The TNF- $\alpha$  concentration in the 3 h, 6 h, 12 h, and 24 h groups increased significantly when compared with that in the control group; **C**, The TNF- $\alpha$  concentration in the 3 h, 6 h, 12 h, and 24 h groups increased significantly when compared with that in the control group; **D**, The TNF- $\alpha$  concentration in the 3 h, 6 h, 12 h, and 24 h groups increased significantly when compared with that in the control group. \*represents  $p < 0.05$  based on a comparison with that in 0 h group.

**Table II.** Scores of the ultrastructure of the mitochondria in the astrocytes of the cerebral cortex of the rats in various experimental groups ( $\bar{x} \pm s$ ).

Group	No. of cases	Mitochondria of Different Levels (%)			No. of mitochondria
		0 Point	1 Point	2 Points	
0 h Group	10	88.34±1.58	1.13±0.46	0.37±1.01	309
6 h Group	10	94.56±1.14	2.97±0.86 <sup>▲*</sup>	0.87±1.21	342
12 h Group	10	94.39±0.56	1.78±1.21	0.49±1.23	332
24 h Group	10	95.78±0.31	1.49±0.35	1.12±0.53	331
F value		2.938	3.450	0.244	
p value		0.047	0.021	0.793	

\* $p < 0.05$  compared with 0 h group. <sup>▲</sup> $p < 0.05$  compared with 12 h group. <sup>▲</sup> $p < 0.05$  compared with 24 h group.

structure score of 3 points and 4 points) were discovered (Figures 2, 3 and Table II).

#### **mRNA Expression of PGC-1 $\alpha$ , NRF-1, NRF-2 $\alpha$ , NRF-2 $\beta$ , and TFAM**

It was found that the concentrations of PGC-1 $\alpha$  mRNA in the 6 h and 12 h groups increased significantly when compared with that in the 0 h group and the difference was statistically significant ( $p < 0.05$ ); there was no significant difference in the astrocytes of the cerebral cortex of the rats between the 24 h group and the 0 h group (Figure 4A); the concentrations of NRF-1 mRNA in the 6 h and 12 h groups increased significantly when compared with that in the 0 h group and the difference was statistically significant ( $p < 0.05$ ); there was no significant difference in the astrocytes of the cerebral cortex of the rats between the 24 h group and the 0 h group (Figure 4B); The concentrations of NRF-2 $\alpha$  mRNA in the 6 h group and the 12 h group increased significantly when compared with that in the 0 h group and the difference was statistically significant ( $p < 0.05$ ); there was no statistically significant difference in the astrocytes of the cerebral cortex of the rats between the 24 h group and the 0 h group (Figure 4C); The concentrations of NRF-2 $\beta$  mRNA in the 6 h group and the 12 h group increased significantly when compared with that in the 0 h group and the difference was statistically significant ( $p < 0.05$ ); there was no statistically significant difference in the astrocytes of the cerebral cortex of the rats between the 24 h group and the 0 h group (Figure 4D); The concentration of TFAM mRNA in the 6 h group, 12 h group, and 24 h group increased significantly when compared with that in the 0 h group. The difference was statistically significant ( $p < 0.05$ ) (Figure 4E).

#### **Protein Expression of PGC-1 $\alpha$ , NRF-1, NRF-2 $\alpha$ , NRF-2 $\beta$ , and TFAM**

The concentration of PGC-1 $\alpha$  protein in the 6 h group and 12 h group increased significantly when compared with that in the 0 h group. The difference was statistically significant ( $p < 0.05$ ). There was no statistically significant difference between the 24 h group and the 0 h group. The concentrations of NRF-1 protein in the 6 h and 12 h groups increased significantly when compared with that in the 0 h group and the difference was statistically significant ( $p < 0.05$ ); there was no statistical difference between the 24 h group and 0 h group. The concentrations of PGC-1 $\alpha$  in the 6 h group and 12 h group increased significantly when compared with that in the 0 h group and the difference was statistically significant ( $p < 0.05$ ). There was no significant difference in the concentration of the NRF-2 $\alpha$  protein in the astrocytes in the cerebral cortex of the rats between the 24 h group and 0 h group. The concentrations of the NRF-2 $\alpha$  protein in the 6 h and 12 h groups increased significantly when compared with that in the 0 h group and the difference was statistically significant ( $p < 0.05$ ); there was no significant difference in the concentration of the NRF-2 $\beta$  protein in the astrocytes in the cerebral cortex of the rats between the 24 h group and 0 h group. The concentrations of the NRF-2 $\beta$  protein in the 6 h and 12 h groups increased significantly when compared with that in the 0 h group and the difference was statistically significant ( $p < 0.05$ ) (Figure 5).

#### **Protein expression of OPAI and DRPI**

OPAI was located in the space between the inner and outer membranes of the mitochondria. It played an important role in regulating fusion of the inner membrane of the mitochondrion. Based on the analysis, it was discovered that the con-

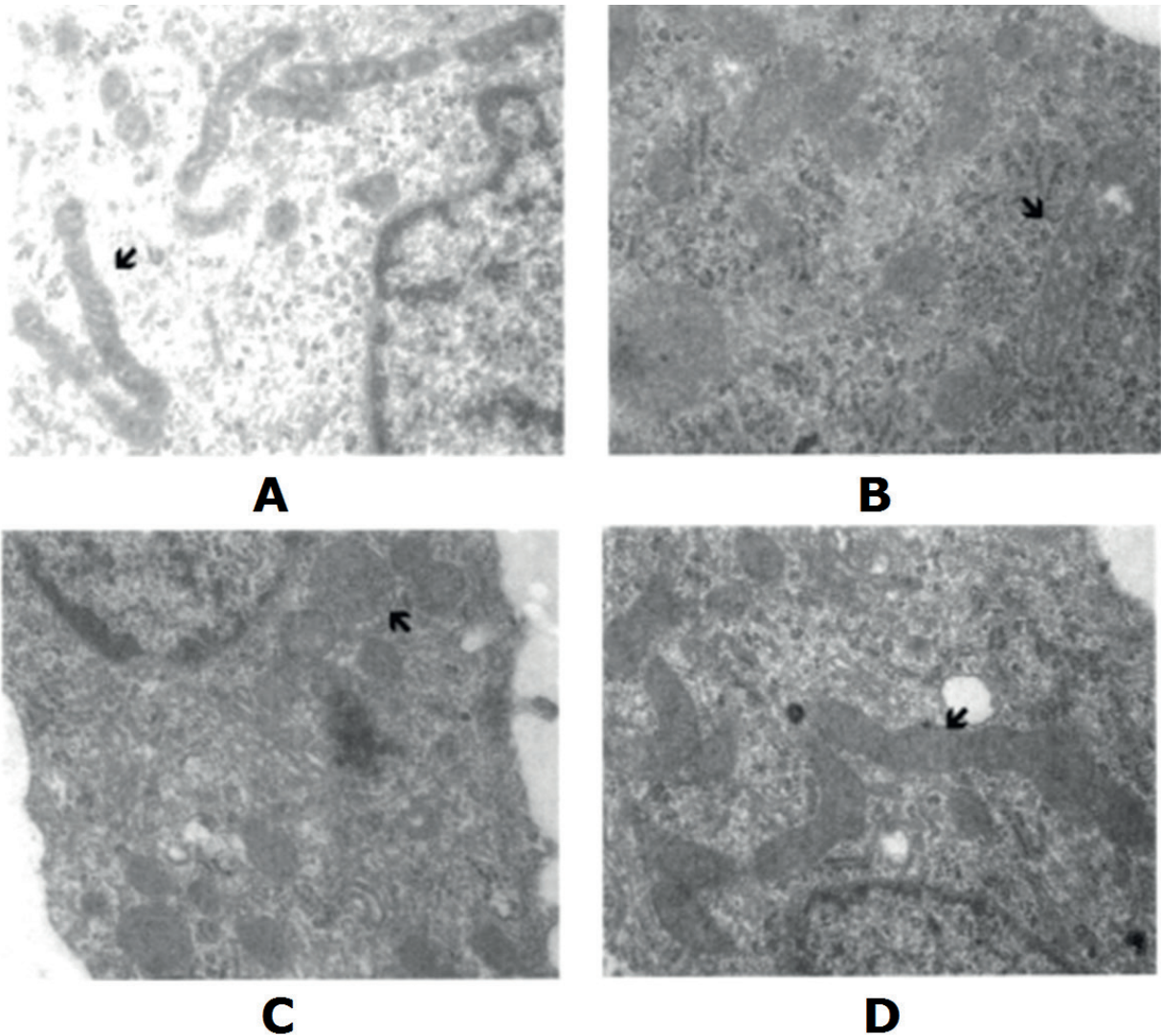


**Figure 3.** Transmission electron microscope image ( $\times 400$ ) for mitochondria in the astrocytes of the cerebral cortex of the rats in various experimental groups. **A**, 0 h group (normal control group): the mitochondria had a normal mitochondrial structure; the crista was clear without structural damage; **B**, 6 h group (sepsis group): The mitochondria were mildly swollen; the electron density of the matrix slightly decreased; no mitochondrial membrane was structurally damaged; **C**, 12 h (sepsis group): the mitochondrial structure was mildly damaged; the mitochondria were mildly swollen; the matrix density decreased slightly; no mitochondrial membrane was structurally damaged; **D**, 24 h group (sepsis group): the mitochondrial structure was normal. The crista was clear without structural damage.

centrations of the OPAI protein in the 6 h and 12 h groups increased significantly when compared with that in the 0 h group and the difference was statistically significant ( $p < 0.05$ ); there was no statistically significant difference in OPAI protein concentration between the 24 h group and the 0 h group; the concentrations of the DRPI protein in the 6 h and 12 h groups increased significantly when compared with that in the 0 h group ( $p < 0.05$ ). There was no statistical difference in the DRPI protein concentration between the 24 h group and the 0 h group (Figure 6).

## Discussion

Based on further in-depth laboratory and clinical research on SAE, clinicians generally have recognized the complexity pathogenesis of SAE. It is the most common nervous system complications influencing the prognosis of the sepsis patients. The sepsis cell models play an important role in studying the pathological and physiological changes of certain cells in the organs with damaged dysfunctions arising from sepsis<sup>24</sup>. Combined use of LPS and IFN- $\gamma$  for astrocytes is better than



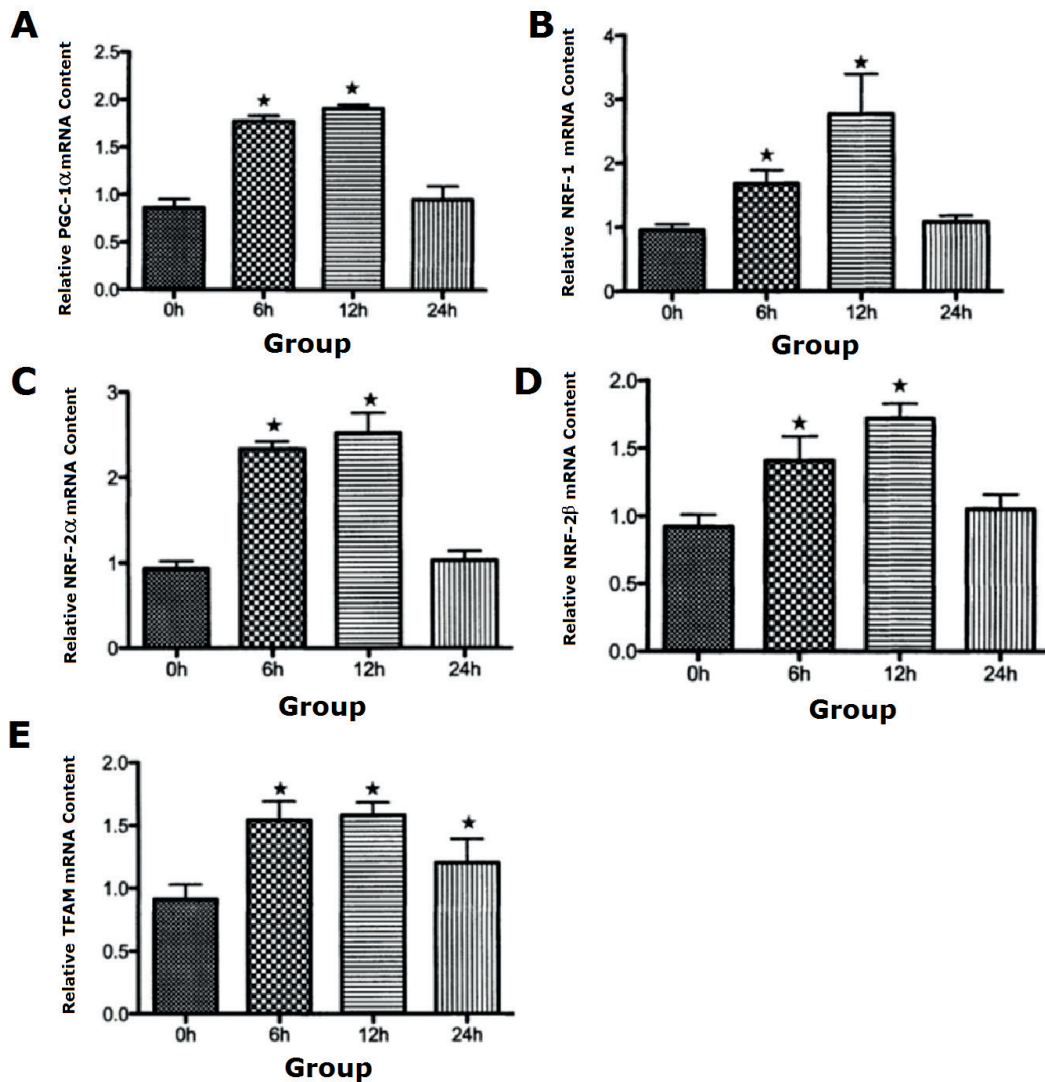


**Figure 4.** Comparison of expression of transcriptional levels of PGC-1 $\alpha$ , NRF-1, NRF-2 $\alpha$ , NRF-2 $\beta$ , and TFAM in the astrocytes of the cerebral cortex of the rats ( $\bar{x} \pm s$ ). **A**, The concentrations of PGC-1 $\alpha$  mRNA in the 6 h and 12 h groups increased significantly when compared with that in the 0 h group; **B**, The concentrations of NRF-1 mRNA in the 6 h and 12 h groups increased significantly when compared with that in the 0 h group ( $p < 0.05$ ); **C**, The concentrations of NRF-2 $\alpha$  mRNA in the 6 h and 12 h groups increased significantly when compared with that in the 0 h group ( $p < 0.05$ ); **D**, The concentrations of NRF-2 $\beta$  mRNA in the 6 h and 12 h groups increased significantly when compared with that in the 0 h group ( $p < 0.05$ ); **E**, The concentrations of TFAM mRNA in the 6 h group, 12 h group, and 24 h group increased significantly when compared with that in the 0 h group ( $p < 0.05$ ).

sole use of LPS or IFN- $\gamma$  in simulating the stimulation effect of the *in vivo* sepsis environment on the astrocytes<sup>25</sup>. We have detected the changes in TNF- $\alpha$  and IL-6 in the culture medium for astrocytes after co-incubation of LPS, IFN, and the astrocytes of the cerebral cortex of the rats, which can reflect the inflammatory reaction degrees. We have also detected the changes in the concentrations of NO in the culture medium for astrocytes and ROS in the astrocytes, which can reflect the

oxidation-nitridation stress degrees. The research enables us to have a clear understanding of the establishment of the models of sepsis astrocytes. Regulation of the mitochondrial biogenesis is a very complex process. Multiple cell nucleus and mitochondrial regulatory factors jointly participate in the mitochondrial biogenesis regulation. The mitochondrial biogenesis refers to growth and fission of existing mitochondria<sup>26</sup>. TFAM promotes the transcription and replication of the mitochon-



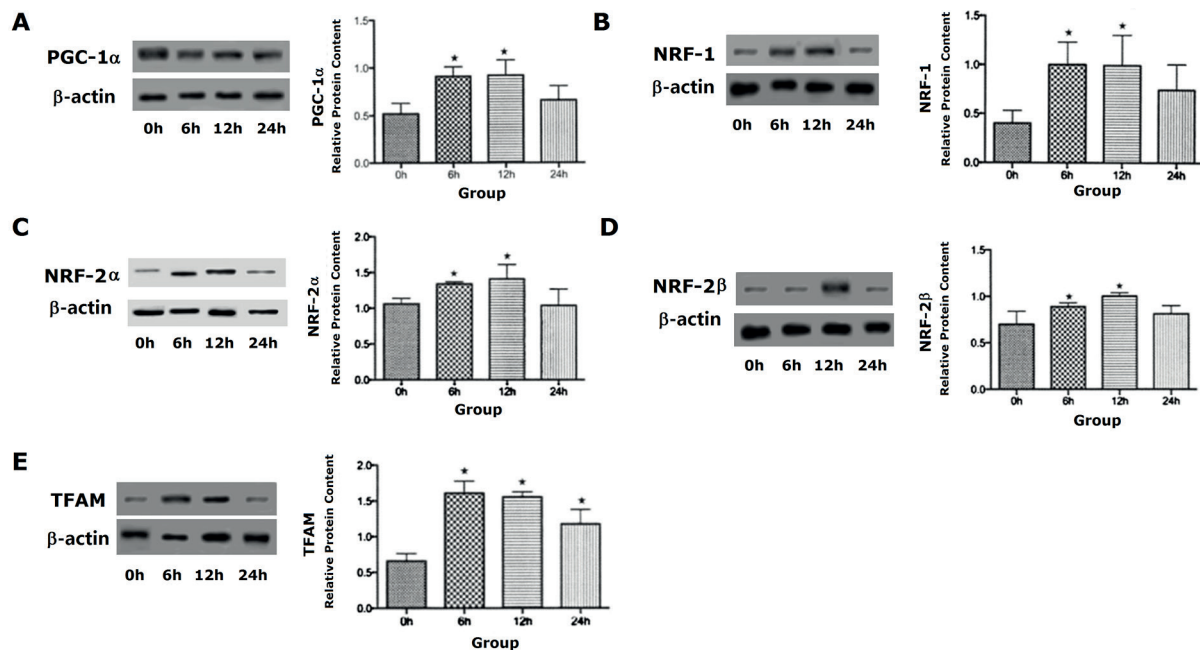


**Figure 5.** Comparison of expression of translational levels (total protein) of PGC-1 $\alpha$ , NRF-1, NRF-2 $\alpha$ , NRF-2 $\beta$ , and TFAM in the astrocytes of the cerebral cortex of the Rats in various experimental groups. **A**, The concentrations of PGC-1 $\alpha$  protein in the 6 h group and 12 h group increased significantly when compared with that in the 0 h group and the difference was statistically significant ( $p < 0.05$ ); **B**, The concentrations of the NRF-1 protein in the 6 h and 12 h group increased significantly when compared with that in the 0h group and the difference was statistically significant ( $p < 0.05$ ); **C**, The concentrations of PGC-1 $\alpha$  protein in the 6 h group and 12 h group increased significantly when compared with that in the 0 h group. The difference was statistically significant ( $p < 0.05$ ); **D**, The concentrations in the 6 h and 12 h groups increased significantly when compared with that in the 0h group and the difference was statistically significant ( $p < 0.05$ ); **E**, The concentrations of the TFAM protein in the 6 h group, 12 h group, and 24 h group increased significantly when compared with that in the 0 h group.

drial DNA and participates in maintaining and stabilizing the mitochondrial DNA structure. It is bound at the upstream recognition sites of the light strand promoter (LSP) and the heavy strand promoter (HSP) of the mitochondrial DNA through specificity for stimulating the DNA transcription<sup>27</sup> NRF-2 can regulate the expression of 10 types of nuclear encoded cytochrome oxidase subunits<sup>28</sup>. A great deal of research has shown that transcribing the assisted activated factor PGC-1 $\alpha$  is the main regulatory factor of mitochondrial biogenesis in mammals. PGC-1 $\alpha$  can activate the mitochondrial uncoupling protein 1(UCP-1)<sup>29</sup> by the interaction between the  $\gamma$  nuclear hormone receptor peroxisome proliferator-activated receptor  $\gamma$  (PPAR- $\gamma$ ) and the thyroid hormone receptors. We have not only detected the PGC-1 $\alpha$  concentration in the total lysis solution of the cellular protein but also detected the PGC-1 $\alpha$  concentration in the nuclear protein. We have found that the transcriptional and translational levels (total protein) of PGC-1 $\alpha$ , NRF-1, NRF-2 $\alpha$ , NRF-2 $\beta$ , and TFAM in the astrocytes of the cerebral cortex of the rats in the 6 h and 12 h groups increase significantly when compared with those

in the control group and the nucleoprotein levels of PGC-1 $\alpha$  in the astrocytes of the cerebral cortex of the rats in the 6 h and 12 h groups increase significantly when compared with those in the control group, indicating that the mitochondrial biogenesis of the astrocytes increases at the two points in time. The transcriptional and translational levels of TFAM (total protein) increase significantly when compared with those in the control group. The research does not involve the factors that trigger increased mitochondrial biogenesis of the cerebral cortex of the rats and related transduction pathways. We only study the changes in the mitochondrial biogenesis, mitochondrial fusion, and fission of the cerebral cortex in *in vitro* sepsis. As the *in vivo* environment is more complex and has more influencing factors, the research requires further *in vivo* experiments for demonstration.

## Conclusions

The experimental sepsis conditions can cause a minor injury of the ultrastructure of the mito-

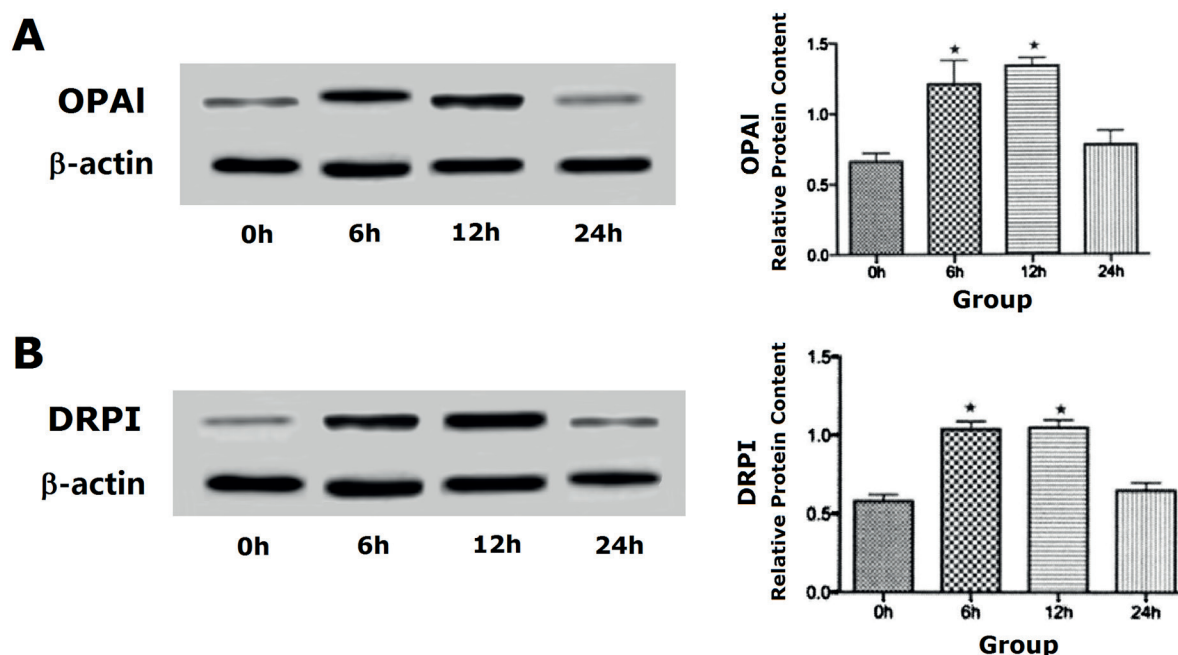


**Figure 6.** Expression of translational levels of OPAI and DRPI in the astrocytes of the cerebral cortex of the rats in various experimental groups. **A**, The concentrations of the OPAI protein in the 6 h and 12 h group increased significantly when compared with that in the 0 h group and the difference was statistically significant ( $p < 0.05$ ); **B**, the concentrations of the DRPI protein in the 6 h group and 12 h group increased significantly when compared with that in the 0 h group and the difference was statistically significant ( $p < 0.05$ ).

chondria in the astrocytes of the cerebral cortex of the rats. The biogenesis of the mitochondria in the astrocytes of the cerebral cortex of the rats was strengthened to cater for the increased demand for energy of the astrocytes under the sepsis conditions and finally recover the ultrastructure of the mitochondria with a minor injury. In response to the increased mitochondrial biogenesis, the activities of the mitochondrial fusion and fission of the astrocytes of the cerebral cortex of the rats were increased.

#### Conflict of interest

The authors declare no conflicts of interest.

#### References

- 1) KARNATOVSKAIA LV, FESTIC E. Sepsis: a review for the neurohospitalist. *Neurohospitalist* 2012; 2: 144-153.
- 2) JUNG SM, MOON SJ, KWOK SK, JU JH, PARK KS, PARK SH, KIM HY. Posterior reversible encephalopathy syndrome in Korean patients with systemic lupus erythematosus: risk factors and clinical outcome. *Lupus* 2013; 22: 885-891.
- 3) CARRILHO PE, SANTOS MB, PIASECKI L, JORGE AC. Marchiafava-Bignami disease: a rare entity with a poor outcome. *Rev Bras Ter Intensiva* 2013; 25: 68-72.
- 4) DENG YY, FANG M, ZHU GF, ZHOU Y, ZENG HK. Role of microglia in the pathogenesis of sepsis-associated encephalopathy. *CNS Neurol Disord Drug Targets* 2013; 12: 720-725.
- 5) TAYLOR NJ, MANAKKAT VG, ABELES RD, AUZINGER G, BERNAL W, MA Y, WENDON JA, SHAWCROSS DL. The severity of circulating neutrophil dysfunction in patients with cirrhosis is associated with 90-day and 1-year mortality. *Aliment Pharmacol Ther* 2014; 40: 705-715.
- 6) PIERRAKOS C, ATTOU R, DECORTE L, KOLYVIRAS A, MALINVERNI S, GOTTIGNIES P, DEVRIENDT J, DE BELS D. Transcranial doppler to assess sepsis-associated encephalopathy in critically ill patients. *BMC Anesthesiol* 2014; 14: 45.
- 7) WANG GB, NI YL, ZHOU XP, ZHANG WF. The AKT/mTOR pathway mediates neuronal protective effects of erythropoietin in sepsis. *Mol Cell Biochem* 2014; 385: 125-132.
- 8) EPSTEIN Y, ROBERTS WO, GOLAN R, HELED Y, SORKINE P, HALPERN P. Sepsis, septic shock, and fatal exertional heat stroke. *Curr Sports Med Rep* 2015; 14: 64-69.
- 9) WANG H, YAN WJ, ZHANG JL, ZHANG FY, GAO C, WANG YJ, BOND LW, TAO L. Adiponectin partially rescues

- high glucose/high fat-induced impairment of mitochondrial biogenesis and function in a PGC-1 $\alpha$  dependent manner. *Eur Rev Med Pharmacol Sci* 2017; 21: 590-599.
- 10) MILANESE M, GIRIBALDI F, MELONE M, BONIFACINO T, MUSANTE I, CARMINATI E, ROSSI PI, VERGANI L, VOCI A, CONTI F, PULITI A, BONANNO G. Knocking down metabotropic glutamate receptor 1 improves survival and disease progression in the SOD1(G93A) mouse model of amyotrophic lateral sclerosis. *Neurobiol Dis* 2014; 64: 48-59.
  - 11) LI H, WANG X, ZHANG N, GOTTIPATI MK, PARPURA V, DING S. Imaging of mitochondrial Ca<sup>2+</sup> dynamics in astrocytes using cell-specific mitochondria-targeted GCaMP5G/6s: mitochondrial Ca<sup>2+</sup> uptake and cytosolic Ca<sup>2+</sup> availability via the endoplasmic reticulum store. *Cell Calcium* 2014; 56: 457-466.
  - 12) WANG Y, CHEN Z, ZHANG Y, FANG S, ZENG Q. Mitochondrial biogenesis of astrocytes is increased under experimental septic conditions. *Chin Med J (Engl)* 2014; 127: 1837-1842.
  - 13) LEMIRE J, AUGER C, MAILLOUX R, APPANNA VD. Mitochondrial lactate metabolism is involved in antioxidative defense in human astrocytoma cells. *J Neurosci Res* 2014; 92: 464-475.
  - 14) UGBODE CI, HIRST WD, RATTRAY M. Neuronal influences are necessary to produce mitochondrial co-localization with glutamate transporters in astrocytes. *J Neurochem* 2014; 130: 668-677.
  - 15) TAXIN ZH, NEYMOTIN SA, MOHAN A, LIPTON P, LYTTON WW. Modeling molecular pathways of neuronal ischemia. *Prog Mol Biol Transl Sci* 2014; 123: 249-275.
  - 16) PEHAR M, BEESON G, BEESON CC, JOHNSON JA, VARGAS MR. Mitochondria-targeted catalase reverts the neurotoxicity of hSOD1G(9)(3)A astrocytes without extending the survival of ALS-linked mutant hSOD1 mice. *PLoS One* 2014; 9: e103438.
  - 17) DARBINIAN N, KHALILI K, AMINI S. Neuroprotective activity of pDING in response to HIV-1 Tat. *J Cell Physiol* 2014; 229: 153-161.
  - 18) XU T, FAN X, TAN Y, YUE Y, CHEN W, GU X. Expression of PHB2 in rat brain cortex following traumatic brain injury. *Int J Mol Sci* 2014; 15: 3299-3318.
  - 19) RAMA RK, NORENBURG MD. Glutamine in the pathogenesis of hepatic encephalopathy: the trojan horse hypothesis revisited. *Neurochem Res* 2014; 39: 593-598.
  - 20) DIENEL GA. Astrocytic energetics during excitatory neurotransmission: What are contributions of glutamate oxidation and glycolysis? *Neurochem Int* 2013; 63: 244-258.
  - 21) NOE N, DILLON L, LELLEK V, DIAZ F, HIDA A, MORAES CT, WENZ T. Bezafibrate improves mitochondrial function in the CNS of a mouse model of mitochondrial encephalopathy. *Mitochondrion* 2013; 13: 417-426.
  - 22) CASARIN A, MCAULEY DF, PAGE VJ. Statins exposure and delirium risk: a winning association?\*. *Crit Care Med* 2014; 42: 1955-1957.
  - 23) HERNANDES MS, D'AVILA JC, TREVELIN SC, REIS PA, KINJO ER, LOPES LR, CASTRO-FARIA-NETO HC, CUNHA FO, BRITTO LR, BOZZA FA. The role of Nox2-derived ROS in the development of cognitive impairment after sepsis. *J Neuroinflammation* 2014; 11: 36.
  - 24) CHAKKARAPANI E, DAVIS J, THORESEN M. Therapeutic hypothermia delays the C-reactive protein response and suppresses white blood cell and platelet count in infants with neonatal encephalopathy. *Arch Dis Child Fetal Neonatal Ed* 2014; 99: F458-F463.
  - 25) SU CM, CHENG HH, TSAI TC, HSIAO SY, TSAI NW, CHANG WN, LIN WC, CHENG BC, SU YJ, CHANG YT, CHIANG YF, KUNG CT, LU CH. Elevated serum vascular cell adhesion molecule-1 is associated with septic encephalopathy in adult community-onset severe sepsis patients. *Biomed Res Int* 2014; 2014: 598762.
  - 26) CHUNG HJ, KIM JD, KIM KH, JEONG NY. G protein-coupled receptor, family C, group 5 (GPRC5B) down-regulation in spinal cord neurons is involved in neuropathic pain. *Korean J Anesthesiol* 2014; 66: 230-236.
  - 27) SPANAKI C, KOTZAMANI D, PETRAKI Z, DRAKOS E, PLAITAKIS A. Heterogeneous cellular distribution of glutamate dehydrogenase in brain and in non-neural tissues. *Neurochem Res* 2014; 39: 500-515.
  - 28) EFTHYMIU A, SHALTOUKI A, STEINER JP, JHA B, HEMAN-ACKAH SM, SWISTOWSKI A, ZENG X, RAO MS, MALIK N. Functional screening assays with neurons generated from pluripotent stem cell-derived neural stem cells. *J Biomol Screen* 2014; 19: 32-43.
  - 29) HONG S, HWANG J, KIM JY, SHIN KS, KANG SJ. Heptachlor induced nigral dopaminergic neuronal loss and Parkinsonism-like movement deficits in mice. *Exp Mol Med* 2014; 46: e80.